



Step-by-step real time monitoring of a catalytic amination reaction†

Cite this: *Chem. Commun.*, 2019, 55, 11727

Received 3rd July 2019,
Accepted 20th August 2019

DOI: 10.1039/c9cc05076k

rsc.li/chemcomm

Gilian T. Thomas,[†] Eric Janusson,[†] Harmen S. Zijlstra[†] and J. Scott McIndoe^{†*}

The multiple reaction monitoring mode of a triple quadrupole mass spectrometer is used to examine the Buchwald–Hartwig amination reaction at 0.1% catalyst loading in real-time using sequential addition of reagents to probe the individual steps in the cycle. This is a powerful new method for probing reactions under realistic conditions.

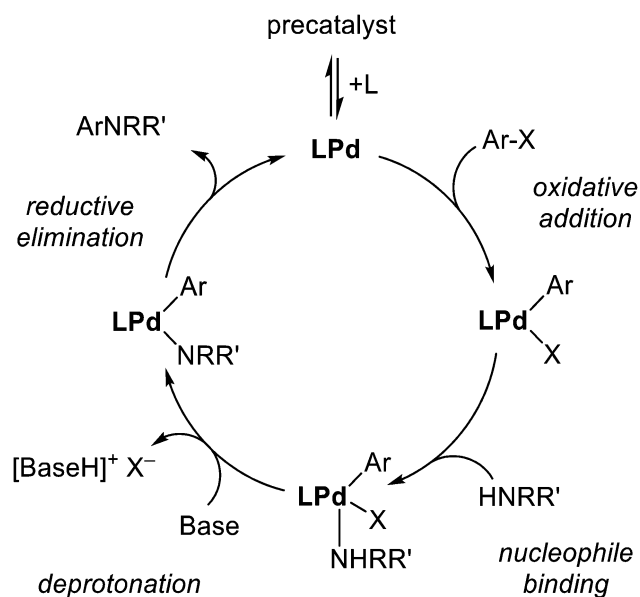
One of the most common ways to form C–N bonds is the Buchwald–Hartwig amination.^{1–4} This versatile palladium-catalyzed cross-coupling between amines and aryl or vinyl halides is widely used and new applications are reported frequently.^{5–14} The reaction mechanism is thought to involve oxidative addition of the aryl halide to Pd(0), coordination of the aniline, deprotonation by base, and reductive elimination of the new C–N bond regenerating the Pd(0) catalyst.^{15–17} Improved understanding of the reaction and observation of the intermediates during this reaction will aid the further development of catalysts and ligands, as well as provide a thorough understanding of substrate effects, allowing optimization of every reaction component.

To date the reaction has been studied by a variety of spectroscopic methods, and the catalytic cycle is fairly well established under certain conditions (Scheme 1), however is not entirely understood due to the complexity of the reaction. For example, use of varying palladium catalysts revealed that the rate limiting step is the reductive elimination,²⁵ and an alternative study employed other substrates to determine that the rate limiting step is the transmetalation.²⁶ It has also been proven that the ligand selected has an effect on the overall yield of the reaction, and the same study found that solvent and base selection have an influence.²⁷

Electrospray ionization mass spectrometry (ESI-MS) has previously been shown to be a valuable tool in studying catalytic reactions.^{28,29} The high sensitivity of the instrument facilitates detection of transient catalytic intermediates which are difficult

to detect using other techniques. Additionally, pressurized sample injection (PSI) allows for simple continuous real-time monitoring of air or moisture sensitive reactions.³⁰

We have recently investigated the activation of Pd₂(dba)₃, a popular catalyst precursor for the Buchwald–Hartwig amination.³¹ We now extend this to monitoring the full Buchwald–Hartwig amination cycle using the commercially available, hydrophilic sulfonated Buchwald-type ligand Na⁺[sPPhos][−] (Fig. 2 inset, from now on represented as L).³² This ligand is advantageous for mechanistic studies involving ESI-MS, as it carries a charge that it can confer to any complex to which it is bound, enabling straightforward detection during analysis.^{33,34} The Buchwald–Hartwig reaction is a challenging target for analysis under normal synthetic conditions, thanks to its high efficiency allowing catalyst loadings as low as 0.1%.³⁵



Scheme 1 Generally accepted mechanism for catalytic amination as mediated by palladium(0) complexes.^{17–24}

Department of Chemistry, University of Victoria, PO Box 1700 STN CSC, Victoria, BC V8W 2Y2, Canada. E-mail: E-mail: mcindoe@uvic.ca

† Electronic supplementary information (ESI) available: Experimental procedures, kinetic analyses, and MS data. See DOI: 10.1039/c9cc05076k

Analysis of a catalytic reaction by PSI-ESI-MS requires all species of interest to be charged, and this can be achieved by using an inherently charged catalyst, by employing a charged substrate, or by modifying the ligand environment to include a charged ligand.²⁹ The last of these approaches was used here. A triple quadrupole mass spectrometer in multiple reaction monitoring (MRM) mode was used in order to detect the low concentrations of catalytically relevant species present in a typical amination reaction. MRM mode applies a double filter to the analysis: the first quadrupole is fixed on a desired m/z value (in the case of the broad Pd-containing isotope patterns analyzed herein, the most abundant isotopomer), it is fragmented using collision-induced dissociation (CID) in the collision cell (not always a quadrupole, despite the name – in the case of this instrument, the collision cell is a hexapole), while the third quadrupole is fixed on a characteristic product ion. Unlike full scan mode, this technique excludes noise and isobaric species (ions appearing at the same m/z), and the signal-to-noise ratio of the analysis is enhanced because the instrument does not spend time scanning the parts of the spectrum of no interest. MRM can be configured such that many different ions can be interrogated on a fast duty cycle, so the effective scan time (time between individual measurements) is of the order of seconds – very fast relative to most spectroscopic methods. In this context “multiple reactions” refers to the unimolecular decomposition reactions (fragmentations) that happen to the selected ions in the collision cell.

MRM has been used extensively to characterize complex biological processes, such as enzymatic catalysis, protein and proteome analysis, and biomarker detection.^{36–39} However, very few applications in organometallic reaction chemistry and homogeneous catalysis have been reported.⁴⁰ Several reaction monitoring studies have been carried out offline using MRM,^{41–44} and several online reaction monitoring studies have been carried out using full scan mode.^{45–47}

In a simple amination reaction, we were able to monitor the formation of key species present in the proposed cycle using MRM mode on a triple quadrupole mass spectrometer (Fig. 1). By adding reagents sequentially, high quality mass spectra of each component could be collected. Identity confirmation of each intermediate was done by comparison of their isotope patterns and exact m/z values compared against calculated values collected on a high resolution hybrid quadrupole-TOF instrument, as well as fragmentation as a result of product ion scans collected on the triple quadrupole instrument. Although each intermediate is observable in the q-TOF instrument, MRM mode on the triple quadrupole instrument holds many advantages over full scan mode as previously mentioned.

The first step of the cycle is transforming the catalyst precursor, $\text{Pd}_2(\text{dba})_3$, into the catalyst resting state. Our previous study of the reaction of $\text{Pd}_2(\text{dba})_3$ with sulfonated phosphines, $[\text{PPh}_2(\text{C}_6\text{H}_4\text{SO}_3)]^-$ and L, using ESI-MS and UV/Vis spectroscopy,³¹ revealed that the only product of catalyst activation in the L case to be $[\text{Pd}(\text{L})(\text{dba})]^-$. This result was replicated here, with a fast and first-order reaction observed with a $t_{1/2} = 0.3$ minutes (Fig. 1, 1–3 minutes).

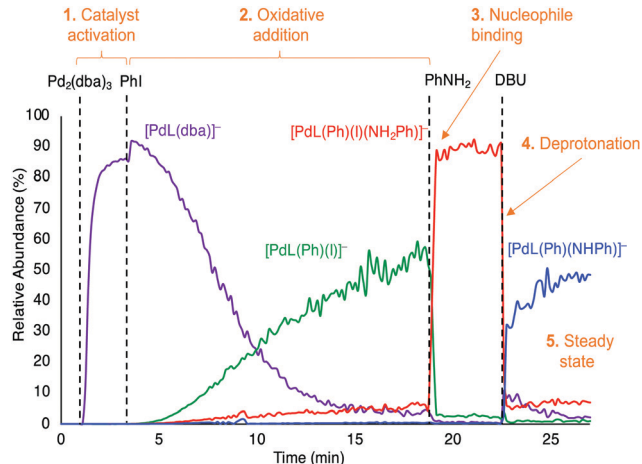


Fig. 1 Sequential addition of reaction components to probe rates of reaction. This data was obtained using MRM scans on a triple-quadrupole mass spectrometer (see ESI,† Table S1 for parameters).

Once catalyst activation was complete, an excess of iodobenzene was added, which resulted in the disappearance of $[\text{Pd}(\text{L})(\text{dba})]^-$ to be replaced predominantly with $[\text{Pd}(\text{L})(\text{Ph})(\text{I})]^-$ (Fig. 1, 3–19 minutes). Small amounts of $[\text{Pd}(\text{L})(\text{Ph})(\text{I})(\text{PhNH}_2)]^-$ were also observed, due to the trace levels of aniline present in commercial PhI.⁴⁸ The differences in rate of $[\text{Pd}(\text{L})(\text{dba})]^-$ consumed vs. $[\text{Pd}(\text{L})(\text{Ph})(\text{I})]^-$ appearing indicated that some other unobserved intermediate was involved. The most obvious candidate for this was the zwitterionic $\text{Pd}(\text{L})(\text{Ph})$, as cationic $[\text{L}_2\text{Pd}(\text{Ar})]^+$ species are a feature of $\text{L}_2\text{Pd}(\text{Ar})(\text{X})$ complexes in polar solvents.⁴⁹ Accordingly, we performed the experiment with SPhos⁵⁰ instead of L (*i.e.* the same ligand, but unsulfonated), and saw the expected production of $[\text{Pd}(\text{SPhos})(\text{Ph})]^+$ in the positive ion mode (Fig. S2, ESI†). The oxidative addition was not particularly rapid, presumably due to the necessity of dba decoordination prior to the reaction taking place.⁵¹ The disappearance of $[\text{Pd}(\text{L})(\text{dba})]^-$ produced a linear plot of the natural log of the abundance of $[\text{Pd}(\text{L})(\text{dba})]^-$ vs. time for the last 10 minutes of the 15 minutes the reaction took to reach equilibrium (Fig. S1, ESI†), and during this period $t_{1/2} = 1.3$ minutes.

Addition of aniline to the reaction mixture caused immediate disappearance of the signal for $[\text{Pd}(\text{L})(\text{Ph})(\text{I})]^-$, to be replaced by $[\text{Pd}(\text{L})(\text{Ph})(\text{I})(\text{PhNH}_2)]^-$ (Fig. 1, 19 minutes). This reaction was faster than the time resolution of the PSI-ESI-MS experiment, which takes some 20 seconds for the solution to move from the reaction flask to the mass spectrometer.⁵² As such, all we can say is that $t_{1/2} < 20$ s. In the positive ion mode (L = SPhos), we did not see the aniline coordinate to the cationic $[\text{PdL}(\text{Ph})]^+$, but we did see a sharp increase in the amount of $[\text{PdL}(\text{Ph})]^+$, suggesting that the aniline does not strongly bind to the cation but does facilitate the displacement of the iodide ligand.

Deprotonation of the bound aniline was just as fast as association of the aniline to the palladium in the previous step, *i.e.* a $t_{1/2}$ of <20 seconds (Fig. 1, 22.5 minutes). The product was $[\text{PdL}(\text{Ph})(\text{NHPh})]^-$, *i.e.* the deprotonation was concomitant with iodide loss. Note that the immediate product of deprotonation of $[\text{PdL}(\text{Ph})(\text{I})(\text{NH}_2\text{Ph})]^-$ would be $[\text{PdL}(\text{Ph})(\text{I})(\text{NHPh})]^{2-}$, however this species was not observed.

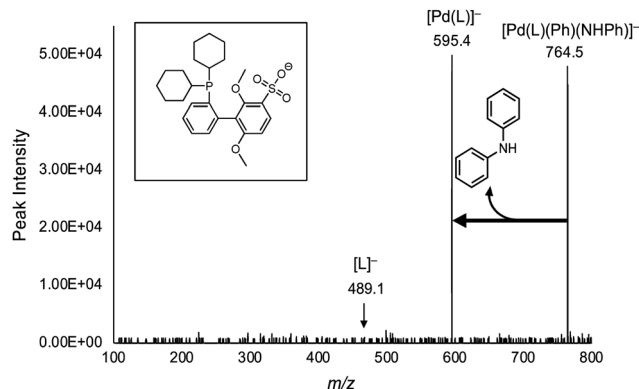


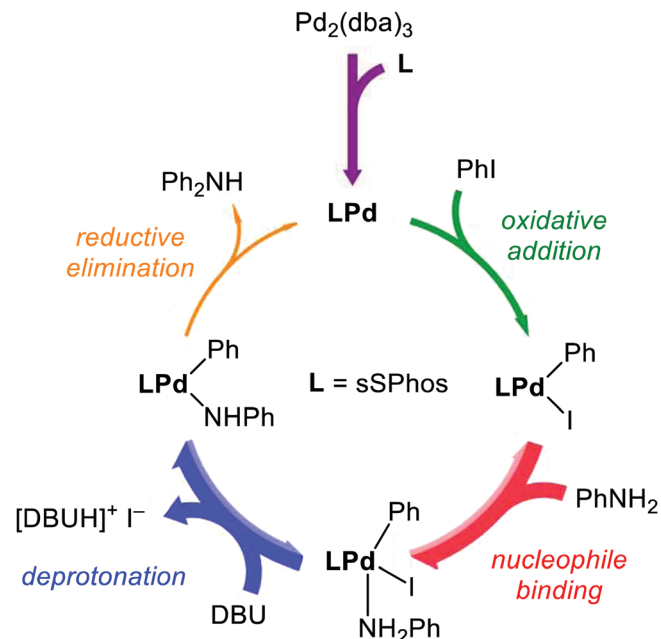
Fig. 2 Product ion mass spectrum of $[\text{Pd}(\text{L})(\text{Ph})(\text{NHPh})]^-$ obtained on a triple quadrupole mass spectrometer. Energetic gas-phase collisions between $[\text{Pd}(\text{L})(\text{Ph})(\text{NHPh})]^-$ and argon atoms ($\text{CE} = 5 \text{ V}$) results in the exclusive formation of $[\text{Pd}(\text{L})]^-$ via loss of reductively eliminated HNPh_2 . Left inset: Structure of $[\text{L}]^-$ ($[\text{sSPhos}]^-$).

Selection of DBU as the base in this reaction prevents formation of NaI species which have been shown to have an inhibitory effect on the reaction.^{27,53} Additionally, performing the reaction in a stepwise fashion rather than ‘one-pot’, prevents observation of base-bound intermediates previously reported, whereby the resting state was determined to be a DBU-bound species after the oxidative addition.⁵⁴ Thus the stepwise catalytic cycle has an alternate steady state, discernible in real-time by mass spectrometry.

After addition of base, the amount of $[\text{PdL}(\text{Ph})(\text{NHPh})]^-$ did not change significantly in the following 30 minutes or so (Fig. 2, first few minutes of this process only shown from 23 minutes). A small amount of $[\text{Pd}(\text{L})(\text{dba})]^-$ was regenerated after addition of base, suggesting some turnover of the reaction was occurring, though $[\text{PdL}(\text{Ph})(\text{NHPh})]^-$ was the dominant catalytically-relevant species and is therefore assigned as the catalyst resting state. Because reductive elimination is a unimolecular decomposition, the transformation could be simulated in the gas phase using collision-induced dissociation (CID).³³ This reaction has the benefit of being able to be performed in isolation from any other solution components, and is therefore uncomplicated by further reactivity. Collisions with argon gas resulted exclusively in reductive elimination of Ph_2NH , with no ligand dissociation observed at all (Fig. 2).

Using reaction calorimetry, this step was previously established to be rate-limiting in triarylamine formation via C–N coupling due to the low nucleophilicity of diarylamines.⁵⁵ However, it was found that the catalytic cycle is in a steady state at $[\text{Pd}(\text{L})(\text{Ph})(\text{NHPh})]^-$ in the formation of diarylamine due to the stepwise addition, as mentioned in the previous section.

Real-time analysis of the Buchwald–Hartwig amination reaction using a triple quadrupole ESI mass spectrometer in multiple reaction monitoring mode revealed rate information on each individual step of the cycle. These data can be summarized in a single set of traces (Fig. 1), and as a catalytic cycle (Scheme 2) whereby the weight of the arrows indicates the



Scheme 2 Catalytic cycle with arrows weighted by relative rate constants of each reaction.⁵⁶

relative magnitude of the (pseudo) first order rate constant of each elementary step in the cycle.

Overall, online reaction monitoring using pressurized sample infusion electrospray ionization mass spectrometry (PSI-ESI-MS) is a viable and powerful method of catalytic mechanism analysis. This is the first reported instance of using multiple reaction monitoring (MRM) scans to observe and quantify catalytically relevant species in real-time. Relative rates of reaction were elucidated, and it was found that the resting state is the $[\text{Pd}(\text{L})(\text{Ph})(\text{NHPh})]^-$ species in the formation of diphenylamine via coupling iodobenzene and aniline.

Conflicts of interest

There are no conflicts to declare.

Notes and references

- D. S. Surry and S. L. Buchwald, *Chem. Sci.*, 2011, **2**, 27–50.
- H. Christensen, S. Kiil, K. Dam-Johansen, O. Nielsen and M. B. Sommer, *Org. Process Res. Dev.*, 2006, **10**, 762–769.
- I. J. S. Fairlamb, A. R. Kapdi, A. F. Lee, G. P. McGlacken, F. Weissburger, A. H. M. de Vries and L. Schmieder-vande Vondervoort, *Chem. – Eur. J.*, 2006, **12**, 8750–8761.
- B. T. Ingoglia, C. C. Wagen and S. L. Buchwald, *Tetrahedron*, 2019, **75**, 4199–4211.
- P. Ruiz-Castillo and S. L. Buchwald, *Chem. Rev.*, 2016, **116**, 12564–12649.
- A. Gangjee, O. A. Namjoshi, S. Raghavan, S. F. Queener, R. L. Kisliuk and V. Cody, *J. Med. Chem.*, 2013, **56**, 4422–4441.
- L. Wang, H. Neumann, A. Spannenberg and M. Beller, *Chem. – Eur. J.*, 2018, **24**, 2164–2172.
- A. S. Guram, *Org. Process Res. Dev.*, 2016, **20**, 1754–1764.
- C. Valente, M. Pompeo, M. Sayah and M. G. Organ, *Org. Process Res. Dev.*, 2014, **18**, 180–190.
- C. Wiethan, W. C. Rosa, H. G. Bonaccorso and M. Stradiotto, *Org. Biomol. Chem.*, 2016, **14**, 2352–2359.

- 11 M. A. MacLean, E. Diez-Cecilia, C. B. Lavery, M. A. Reed, Y. Wang, D. F. Weaver and M. Stradiotto, *Bioorg. Med. Chem. Lett.*, 2016, **26**, 100–104.
- 12 D. Nandi, R. U. Islam, N. Devi, S. Siwal and K. Mallick, *New J. Chem.*, 2018, **42**, 812–816.
- 13 C. Lombardi, J. Day, N. Chandrasoma, D. Mitchell, M. J. Rodriguez, J. L. Farmer and M. G. Organ, *Organometallics*, 2017, **36**, 251–254.
- 14 P. G. Gildner, A. DeAngelis and T. J. Colacot, *Org. Lett.*, 2016, **18**, 1442–1445.
- 15 K. H. Hoi, S. Çalimsiz, R. D. J. Froese, A. C. Hopkinson and M. G. Organ, *Chem. – Eur. J.*, 2012, **18**, 145–151.
- 16 Y. Sunesson, E. Limé, S. O. Nilsson Lill, R. E. Meadows and P.-O. Norrby, *J. Org. Chem.*, 2014, **79**, 11961–11969.
- 17 M. S. Driver and J. F. Hartwig, *J. Am. Chem. Soc.*, 1997, **119**, 8232–8245.
- 18 R. A. Widenhoefer and S. L. Buchwald, *Organometallics*, 1996, **15**, 2755–2763.
- 19 M. S. Driver and J. F. Hartwig, *J. Am. Chem. Soc.*, 1995, **117**, 4708–4709.
- 20 J. F. Hartwig, S. Richards, D. Barañano and P. Frédéric, *J. Am. Chem. Soc.*, 1996, **118**, 3626–3633.
- 21 A. S. Guram, R. A. Rennels and S. L. Buchwald, *Angew. Chem., Int. Ed. Engl.*, 1995, **34**, 1348–1350.
- 22 J. Louie and J. F. Hartwig, *Tetrahedron Lett.*, 1995, **36**, 3609–3612.
- 23 A. S. Guram and S. L. Buchwald, *J. Am. Chem. Soc.*, 1994, **116**, 7901–7902.
- 24 F. Paul, J. Patt and J. F. Hartwig, *J. Am. Chem. Soc.*, 1994, **116**, 5969–5970.
- 25 J. Louie, P. Frédéric and J. F. Hartwig, *Organometallics*, 1996, **15**, 2794–2805.
- 26 E. V. Vinogradova, B. P. Fors and S. L. Buchwald, *J. Am. Chem. Soc.*, 2012, **134**, 11132–11135.
- 27 B. P. Fors, N. R. Davis and S. L. Buchwald, *J. Am. Chem. Soc.*, 2009, **131**, 5766–5768.
- 28 K. L. Vikse, Z. Ahmadi and J. S. McIndoe, *Coord. Chem. Rev.*, 2014, **279**, 96–114.
- 29 L. P. E. Yunker, R. L. Stoddard and J. S. McIndoe, *J. Mass Spectrom.*, 2014, **49**, 1–8.
- 30 K. L. Vikse, M. P. Woods and J. S. McIndoe, *Organometallics*, 2010, **29**, 6615.
- 31 E. Janusson, H. S. Zijlstra, P. P. T. Nguyen, L. Macgillivray, J. Martelino and J. S. McIndoe, *Chem. Commun.*, 2017, **854**, 854–856.
- 32 K. W. Anderson and S. L. Buchwald, *Angew. Chem., Int. Ed.*, 2005, **44**, 6173–6177.
- 33 K. L. Vikse, M. A. Henderson, A. G. Oliver and J. S. McIndoe, *Chem. Commun.*, 2010, **46**, 7412.
- 34 D. M. Chisholm and J. S. McIndoe, *Dalton Trans.*, 2008, 3933.
- 35 S. Urgaonkar and J. G. Verkade, *J. Org. Chem.*, 2004, **69**, 9135–9142.
- 36 B. Doman and R. Aebbersold, *Science*, 2006, **312**, 212–217.
- 37 S. A. Carr and L. Anderson, *Clin. Chem.*, 2008, **54**, 1749–1752.
- 38 A. J. Norris, J. P. Whitelegge, K. F. Faull and T. Toyokuni, *Biochemistry*, 2001, **40**, 3774–3779.
- 39 A. J. Norris, J. P. Whitelegge, K. F. Faull and T. Toyokuni, *Anal. Chem.*, 2001, **73**, 6024–6029.
- 40 Y. Wang, W.-Y. Lin, K. Liu, R. J. Lin, M. Selke, H. C. Kolb, N. Zhang, X.-Z. Zhao, M. E. Phelps, C. K. F. Shen, K. F. Faull and H.-R. Tseng, *Lab Chip*, 2009, **9**, 2281–2285.
- 41 D. V. Sojic, V. B. Anderlüh, D. Z. Orcic and B. F. Abramovic, *J. Hazard. Mater.*, 2009, **168**, 91–101.
- 42 J. Qiao, X. Sun and L. Zhu, *Rapid Commun. Mass Spectrom.*, 2009, **23**, 1264–1268.
- 43 Q. Zhuo, S. Deng, B. Yang, J. Huang and G. Yu, *Environ. Sci. Technol.*, 2011, **45**, 2973–2979.
- 44 M. W. Lam, C. J. Young and S. A. Mabury, *Environ. Sci. Technol.*, 2005, **39**, 513–522.
- 45 X. Yan, E. Sokol, X. Li, G. Li, S. Xu and R. G. Cooks, *Angew. Chem., Int. Ed.*, 2014, **53**, 5931–5935.
- 46 A. Ray, T. Bristow, C. Whitmore and J. Mosely, *Mass Spectrom. Rev.*, 2018, **37**, 565–579.
- 47 C. Iacobucci, S. Reale and F. DeAngelis, *Angew. Chem., Int. Ed.*, 2016, **55**, 2980–2993.
- 48 Repeated washing with acid was required to reduce aniline contamination to the levels shown. At a catalyst loading of 0.1%, observing aniline binding suggested a contamination level of ~0.1% (ppm).
- 49 L. P. E. Yunker, Z. Ahmadi, J. R. Logan, W. Wu, T. Li, A. Martindale, A. G. Oliver and J. S. McIndoe, *Organometallics*, 2018, **37**, 4297–4308.
- 50 T. E. Barder, S. D. Walker, A. Joseph, R. Martinelli and S. L. Buchwald, *J. Am. Chem. Soc.*, 2005, **127**, 4685–4696.
- 51 P. Weber, A. Biafora, A. Doppiu, H.-J. Bongard, H. Kelm and L. J. Gooßen, *Org. Process Res. Dev.*, 2019, **23**, 1462–1470.
- 52 K. L. Vikse, Z. Ahmadi, J. Luo, N. Van Der Wal, K. Daze, N. Taylor and J. S. McIndoe, *Int. J. Mass Spectrom.*, 2012, **323**, 8–13.
- 53 J. M. Dennis, N. A. White, R. Y. Liu and S. L. Buchwald, *J. Am. Chem. Soc.*, 2018, **140**, 4721–4725.
- 54 J. M. Dennis, N. A. White, R. Y. Liu and S. L. Buchwald, *ACS Catal.*, 2019, **9**, 3822–3830.
- 55 P. L. Arrechea and S. L. Buchwald, *J. Am. Chem. Soc.*, 2016, **138**, 12486–12493.
- 56 J. McFarlane, B. Henderson, S. Donneck and J. S. McIndoe, *ChemRxiv*, 2019, DOI: 10.26434/chemrxiv.8206637.v1.